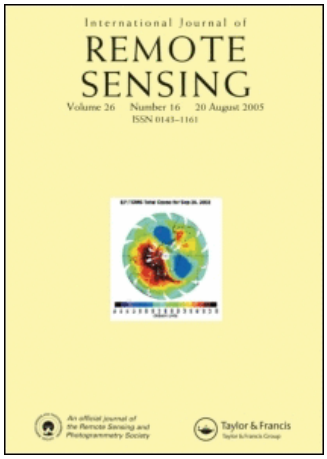


International Journal of Remote Sensing
Publication details, including instructions for authors and subscription information:
http://www.informaworld.com/smpp/title~content=t713722504

# Inter-calibration of the Moderate-Resolution Imaging Spectroradiometer and the AlongTrack Scanning Radiometer-2

C. R. N. Rao [a]; C. Cao [a]; N. Zhang [b]
[a] NOAA/NESDIS/Office of Research and Applications, 5200 Auth Road, Camp Springs, MD 20746-4304, USA.
[b] QSS Group, Inc., 4200 Forbes Blvd, Lanham, MD 20706, USA.

Online Publication Date: 10 May 2003
To cite this Article: Rao, C. R. N., Cao, C. and Zhang, N. (2003) 'Inter-calibration of the Moderate-Resolution Imaging Spectroradiometer and the AlongTrack Scanning Radiometer-2', International Journal of Remote Sensing, 24:9, 1913 - 1924
To link to this article: DOI: 10.1080/01431160210154993
URL: http://dx.doi.org/10.1080/01431160210154993

INT. J. REMOTE SENSING, 2003, VOL. 24, NO. 9, 1913–1924





# Inter-calibration of the Moderate-Resolution Imaging Spectroradiometer and the AlongTrack Scanning Radiometer-2

C. R. N. RAO†, C. CAO*

NOAA/NESDIS/Office of Research and Applications, 5200 Auth Road, Camp Springs, MD 20746-4304, USA

and N. ZHANG

QSS Group, Inc., 4200 Forbes Blvd, Lanham, MD 20706, USA

(*Received 23 July 2001; in final form 8 January 2002*)

**Abstract.** The performance of the on board calibrator for bands 1 ($\approx 0.66\,\mu$m), 2 ($\approx 0.86\,\mu$m) and 4 ($\approx 0.55\,\mu$m) of the Moderate-Resolution Imaging Spectroradiometer (MODIS Terra) has been evaluated by comparison of the top-of-atmosphere (TOA) albedos measured in the three bands over a six-day period with a three-year record of TOA albedos measured in the 0.56, 0.66 and 0.86 $\mu$m channels of the Along-Track Scanning Radiometer-2 (ATSR-2). The albedo measurements were made over two radiometrically stable sites located in the Libyan desert (22°0′ N, 28°30′ E), Sudan, and in the Sonoran desert (32°0′ N, 114°6′ W), Mexico. MODIS Terra albedos are within $\pm 2.5$ per cent of those measured in the corresponding channels of ATSR-2. Analysis of the measurements, and of model-derived albedos in the three channels (bands) of the two instruments, indicates that the MODIS Terra on board calibrator for bands 1, 2 and 4 is functioning as expected, and that either of the two instruments can be used to monitor the in-orbit performance of the other.

## 1. Introduction

Post-launch calibration and inter-calibration of satellite sensors are essential to ensure the accuracy, continuity and viability of long-term records of satellite-derived geophysical products (e.g. columnar aerosols over oceans, aerosol radiative forcing, Normalized Difference Vegetation Index and sea surface temperature), and to ensure the traceability of satellite radiance measurements to the International System of Units (SI units). The geophysical products may be derived either from the same sensor on successive members of a spacecraft series (e.g. Normalized Difference Vegetation Index from the Advanced Very High Resolution Radiometer (AVHRR) on the NOAA polar orbiters), or from different sensors either on the same spacecraft or on different spacecraft (e.g. columnar aerosols from the AVHRR, ATSR-2 and

*Author for correspondence at E/RA1, Rm. 810, WWB, NOAA/NESDIS Office of Research and Applications, 5200 Auth Road, Camp Springs, MD 20746-4304, USA; email: changyong.cao@noaa.gov

†Deceased. 11 May 2001.

*International Journal of Remote Sensing*
ISSN 0143-1161 print/ISSN 1366-5901 online © 2003 Taylor & Francis Ltd
http://www.tandf.co.uk/journals
DOI: 10.1080/01431160210154993

MODIS Terra) (Rao and Chen 1995, Slater *et al.* 1996, Gao 2000). Accordingly, post-launch calibration of satellite sensors, and inter-calibration of the same are considered one of the primary requirements of national and international activities directed towards the study of the atmosphere, land and oceans of Earth, and its climate, such as the World Climate Research Programme (WCRP), the International Geosphere Biosphere Program (IGBP) and the Global Climate, Terrestrial and Ocean Observing Systems (G3OS), to name a few. It is against this background that we wish to present here our evaluation of the performance of the on board calibrator for bands 1 ($\approx$0.66 $\mu$m), 2 ($\approx$0.86 $\mu$m), and 4 ($\approx$0.55 $\mu$m) of MODIS Terra—hereafter referred to as MODIS—using the ATSR-2 as a calibration reference.

## 2. Method

### 2.1. *Sensors*

MODIS is a 36-channel filter radiometer designed for the remote sensing of the composition and structure of the surface of the Earth and the overlying atmosphere. A distinguishing feature of the instrument is the very well-designed on board calibrator for the visible and near-infrared channels (Guenther *et al.* 1996). It was launched on 18 December 1999 aboard the Terra spacecraft into a sun-synchronous, polar orbit at an altitude of 705 km. Terra crosses the equator from north to south at $\approx$10 h 40 m local time. ATSR-2 is a 7-channel filter radiometer with an on board calibrator for the visible and near-infrared channels. It was launched on the ERS-2 spacecraft into a sun-synchronous, polar orbit at an altitude of 824 km on 21 April 1995. ERS-2 crosses the equator from north to south at $\approx$10 h 30 m local time. The performance of the ATSR-2 on board calibrator over a period of three years has been evaluated using vicarious post-launch calibration (Smith *et al.* 2002), and found to be stable (2%).

The sensor characteristics which are relevant to the present study are the equivalent width, the effective wavelength, and the in-band extraterrestrial solar irradiance at mean Earth–Sun distance. The equivalent width $\omega$ (in $\mu$m) is given by:

$$\omega = \int_{\lambda_1}^{\lambda_2} \tau_\lambda d\lambda \tag{1}$$

where $\tau_\lambda$ is the normalized response function of the instrument at the wavelength $\lambda$, $\lambda_1$ and $\lambda_2$ are respectively the lower and upper limits of the spectral interval covered by any given channel. The normalized response function $\tau_\lambda$ is less than one at all wavelengths other than the wavelength at which the instrument has peak response; and it is equal to one at the wavelength of peak response. The extra-terrestrial in band solar irradiance $F$ (in w m$^{-2}$) is given by:

$$F = \int_{\lambda_1}^{\lambda_2} F_{0\lambda} \tau_\lambda d\lambda \tag{2}$$

where $F_{0\lambda}$ is the extraterrestrial solar irradiance at the wavelength $\lambda$. The effective wavelength $\lambda_e$ (in $\mu$m)is given by:

$$\lambda_e = \int_{\lambda_1}^{\lambda_2} \lambda F_{0\lambda} \tau_\lambda d\lambda / F \tag{3}$$

The above characteristics of the different channels of MODIS and ATSR-2 under study are listed in table 1.

Table 1. Sensor characteristics.

| Instrument | Spectral interval ($\mu$m) (50% points) | Equivalent width $\omega$ ($\mu$m) | Effective wavelength $\lambda_e$ ($\mu$m) | In-band solar irradiance $F$ (W m$^{-2}$) |
|---|---|---|---|---|
| MODIS | | | | |
| Band 4 | 0.545–0.565 | 0.019 | 0.555 | 34.6 |
| Band 1 | 0.620–0.670 | 0.041 | 0.646 | 66.4 |
| Band 2 | 0.841–0.876 | 0.039 | 0.856 | 39.4 |
| ATSR-2 | | | | |
| Channel 7 | 0.540–0.560 | 0.018 | 0.556 | 32.6 |
| Channel 6 | 0.650–0.670 | 0.023 | 0.658 | 35.6 |
| Channel 5 | 0.860–0.870 | 0.019 | 0.864 | 18.3 |

2.2. *Model simulations of the upward radiation*

The upward radiation emerging at the top of the atmosphere in bands 1 ($\approx$0.66 $\mu$m), 2 ($\approx$0.86 $\mu$m) and 4 ($\approx$0.55 $\mu$m) of MODIS, and in the 0.56 $\mu$m, 0.66 $\mu$m and 0.86 $\mu$m channels of the ATSR-2, and the corresponding top-of-atmosphere (TOA) albedos, were computed for a very representative set of atmospheric and surface conditions, and of solar illumination and observational geometries, using the LOWTRAN/MODTRAN radiative transfer code (Berk *et al*. 1989). Conforming to the generally prevalent practice in meteorological applications of satellite radiance measurements in the visible and near-infrared regions of the spectrum, we define the TOA albedo A (in per cent) as

$$A = 100\pi I\omega/(F \cos \theta_0) \tag{4}$$

where $I$ is the average radiance (w m$^{-2}$ sr$^{-1}$ $\mu$m$^{-1}$) in the channel of interest, and $\theta_0$ is the solar zenith angle.

In order to obtain reliable estimates of the upward radiation in the MODIS and ATSR-2 channels that would take into account the wavelength dependence of surface reflectance, and of atmospheric effects, we performed the model simulations using an appropriate number (seven to ten depending upon the equivalent width of the sensor) of sub-spectral intervals for the different sensors. Three different cases of the wavelength dependence of surface reflectance were considered in the model simulations, namely, (a) Lambertian surface with pronounced wavelength dependence of reflectance, typified by vegetation with different amounts of chlorophyll; (b) Lambertian surface with reflectance slowly varying with wavelength, typified by soils (deserts); and (c) Lambertian surface with the same reflectance at all wavelengths. Also, as the surface meteorological range changes from 300 km to 23 km to 5 km in the model simulations, the atmosphere changes from purely molecular (or gaseous) to highly turbid, with appreciable amounts of aerosol; the corresponding aerosol normal attenuation optical thickness values are 0, 0.32 and 1.2. We list in table 2 the atmospheric and surface parameters used in the model simulations.

In general, the model simulations of the TOA albedos in the two sensors being inter-calibrated—the reference (i.e. ATSR-2) and candidate (i.e. MODIS) sensors—serve two objectives: (a) to transfer the calibration of the reference sensor to the candidate sensor via radiometrically stable calibration sites when the candidate sensor has no on board calibrator; and (b) to monitor the performance of instruments with on board calibrators, and to serve as a surrogate calibrator in the event of

Table 2. Atmospheric and surface parameters used in the LOWTRAN/MODTRAN model simulations.

| Atmospheric model | Tropical and mid-latitude summer |
|---|---|
| Solar zenith angle | 30, 45, and 60 deg |
| Satellite viewing angle | 0, 15, 30, and 45 deg |
| Relative azimuth angle | 0, 90, and 180 deg |
| Aerosol | Rural |
| Surface meteorological range | 5, 23, and 300 km |

failure of the on board calibrator. The model simulations of the MODIS and ATSR-2 albedos serve the latter objective in the present study. Thus, the regression relationship between the two albedos in the model simulations will be used to estimate the MODIS albedos over the calibration sites (see next section) which in turn will be used to reinforce our findings from the inter-comparison of the measured albedos.

### 2.3. *MODIS and ATSR-2 data*

We inter-compare TOA albedos measured by MODIS and ATSR-2 over two radiometrically stable sites located in the Libyan desert (22°0′ N, 28°30′ E), Sudan, and in the Sonoran desert (32°0′ N, 114°6′ W), Mexico, to evaluate the performance of the on board calibrator of the former. Here radiometric stability implies that the TOA albedo is uniform in time for all practical purposes, and that the small but finite variations of the same in the course of the year are reproduced from one year to the next. The MODIS TOA albedos in bands 1, 2 and 4 for the two desert sites are obtained from cloud free, level lb data. In order to find the appropriate data sets, orbit tracking of the Terra satellite is needed. There are several websites that provide the Terra orbits for a given date, but searching for the orbit near nadir for a given location is rather difficult. Therefore, to speed up the searching process, the software package Satellite Tool Kit (STK) with the appropriate two-line-elements for Terra was used for quickly identifying overpasses for these two sites (http://celestrak.com/NORAD/elements). We consider only albedo measurements made close to the nadir to minimize the impact of azimuthal dependence, if any, of the upward radiation on the inter-comparison of the two instruments; this requirement restricted the number of days on which useable data could be obtained to six between December 2000 and April 2001. Thus, we use data obtained during MODIS overpasses on 29 December 2000, 10 March 2001 and 26 March 2001 for the Libyan desert site; and on 15 December 2000, 12 March 2001 and 28 March 2001 for the Sonoran desert site in the evaluation of MODIS on board calibration. The nadir angle of observation was less than, or equal to 10°. The two sites measured roughly 1 deg (longitude) × 2 deg (latitude).

The ATSR-2 TOA albedo data were collected for the two desert sites over a period of three years (1995–1998); both near-nadir (observation angle $\leqslant 20°$), and along-track (observation angle $> 50°$) measurements are used since the three-year means of the two are within 0.5% of each other. Greater details of data acquisition and processing are given in Smith *et al* (2002). We show in figures 1 and 2 the three-year time series of ATSR-2 albedo measurements over the two sites. It should be noted that several sites in the Libyan desert, including the one used in the present study, have been used by investigators elsewhere in the post-launch calibration of the visible and near-infrared channels of the AVHRR on the NOAA polar orbiters,

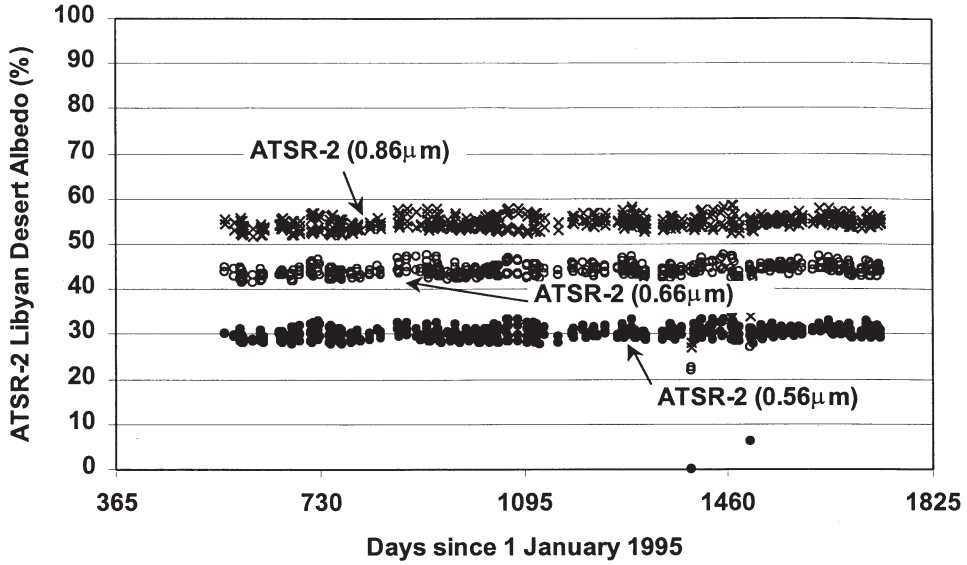


Figure 1. ATSR-2 albedo measurements over the Libyan desert site.

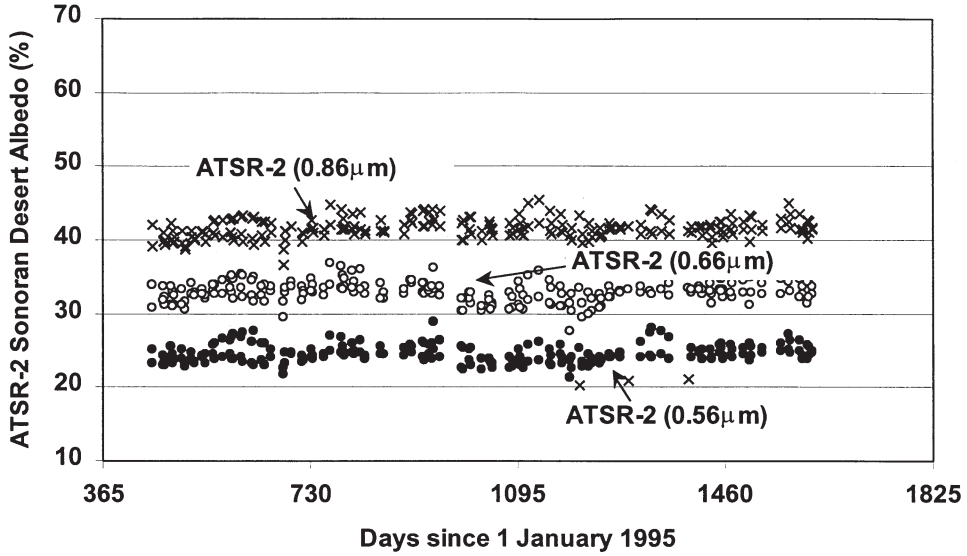


Figure 2. ATSR-2 albedo measurements over the Sonoran desert site.

and the visible sensor on METEOSAT (e.g. Staylor 1990, Kaufman and Holben 1993, Arriaga and Schmetz 1998.)

## 3. Results

### 3.1. *Computations*

We show in figure 3 the normalized response functions (top), and the wavelength dependence of the surface reflection (bottom) that we have used in the model simulations. The vegetation reflectance spectra are for different amounts of chlorophyll (Chl), expressed in mmol $cm^{-2}$ (Gitelson and Merzlyak 1994), and corre-

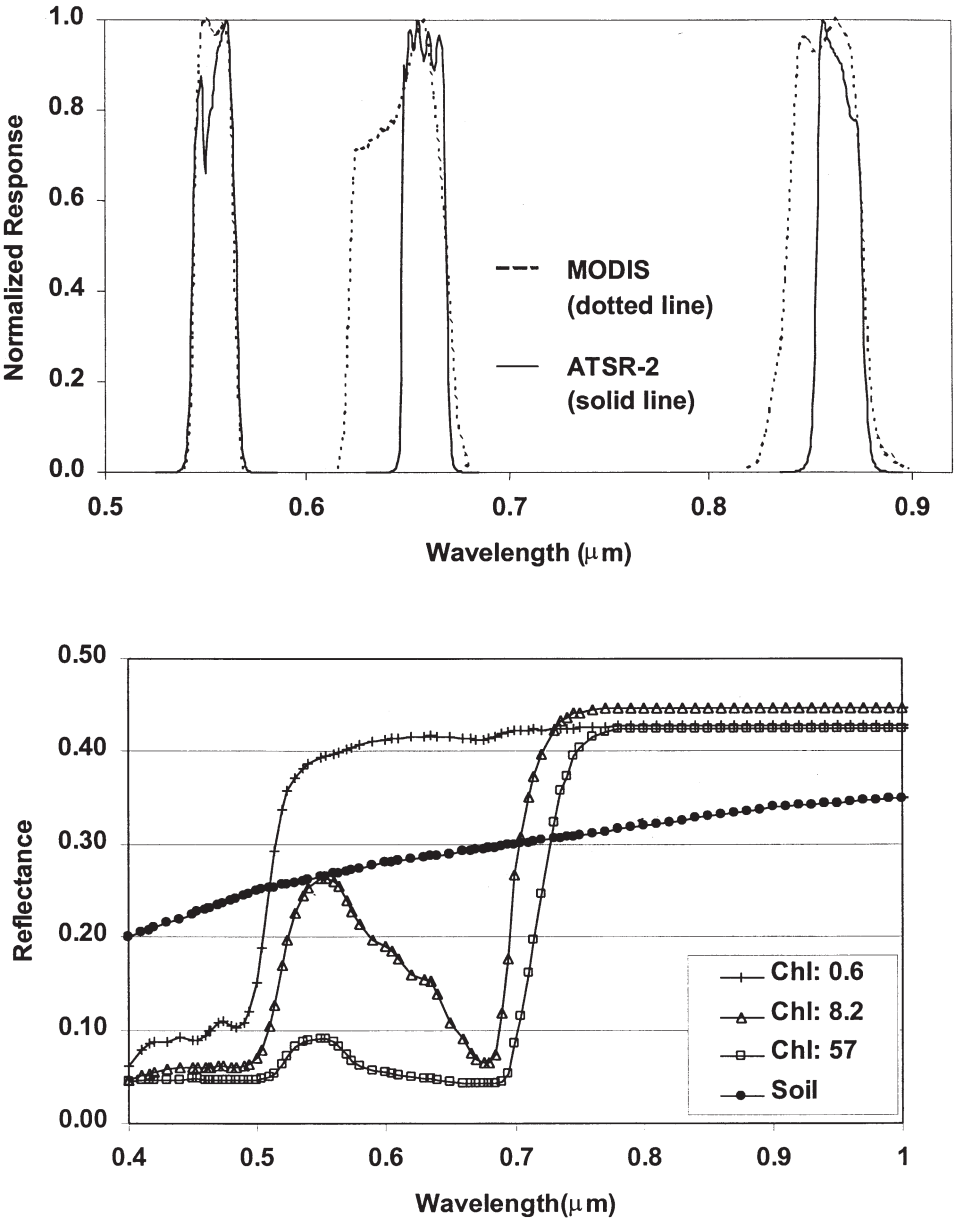


Figure 3. The normalized response functions (top) of the ATSR-2, and MODIS sensors, and typical surface reflectance spectra (bottom).

spond to different stages of growth of vegetation in a generic manner. We use these reflectance spectra only to bring out the impact of the spectral dependence of surface reflection of different degrees on the emergent radiation at the top of the atmosphere; and not to imply that the entire Earth's surface is covered with vegetation.

The very robust inter-relationship amongst the simulated TOA albedos in the different channels of MODIS and ATSR-2 is shown in figures 4, 5 and 6. The high degree of correspondence between the computed albedos measured by the two

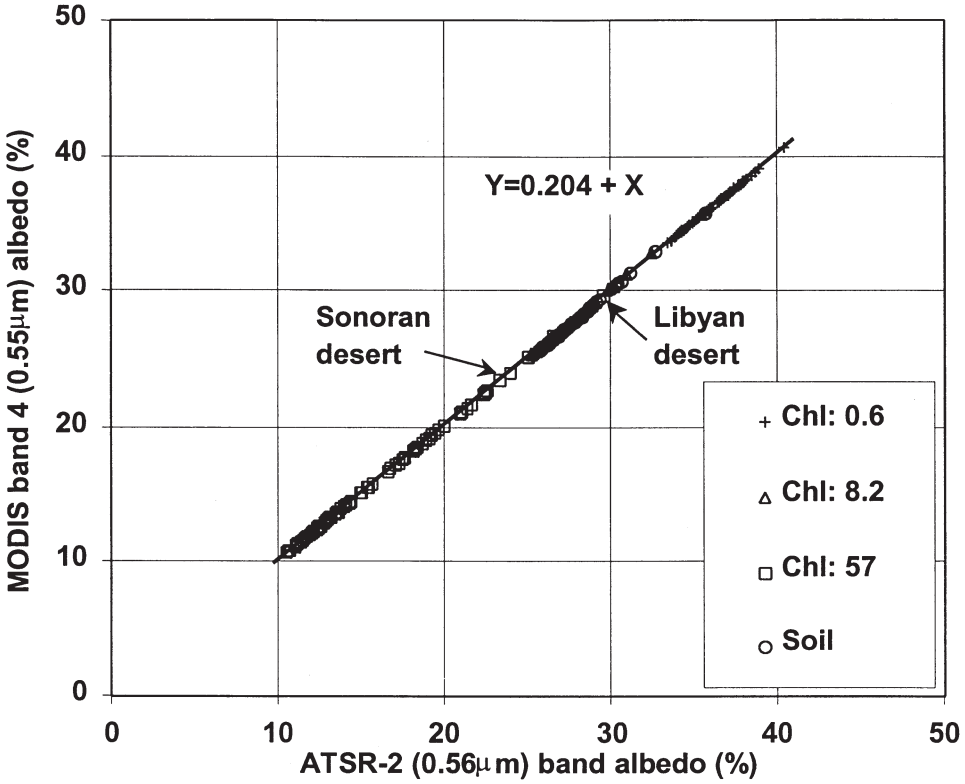


Figure 4. Regression of the computed MODIS band 4 albedo on the computed ATSR-2 0.56 $\mu$m band albedo.

instruments is to be expected since the MODIS and ATSR-2 channels under study are essentially located in the same region of the spectrum; have effective wavelengths which are very close to each other; and the corresponding equivalent widths are comparable (table 1; also figure 3). We list in table 3 the regression relationships between the two albedos; the $R^2$ values for all of these regressions are in excess of 0.98. Assuming that we have no *a priori* knowledge of the albedo that would be measured by MODIS, we estimate its value over the two sites using the regression relationship between the MODIS and ATSR-2 albedos (table 3), and use these estimates to serve as a secondary reference—the first being the ATSR-2—to evaluate the MODIS albedo measurements. Please note that the regression between MODIS and ATSR-2 albedos shown in figures 4, 5 and 6 is based on simulations of hypothetical scenarios for vegetation and soil. In this study, the regression is verified by inter-calibrating the two instruments using the two desert sites, the albedos of which fall within a narrow range as indicated in figures 4, 5 and 6. Although the regression relationship outside the desert albedo range appears to be equally promising, it is subject to further validation and verification.

### 3.2. *Measurements*

We show in table 4 the measured and estimated values of MODIS albedo along with the ATSR-2 albedo for the Libyan and the Sonoran desert sites. The entries in the MODIS 'measured' column are the mean values over at least a few hundred

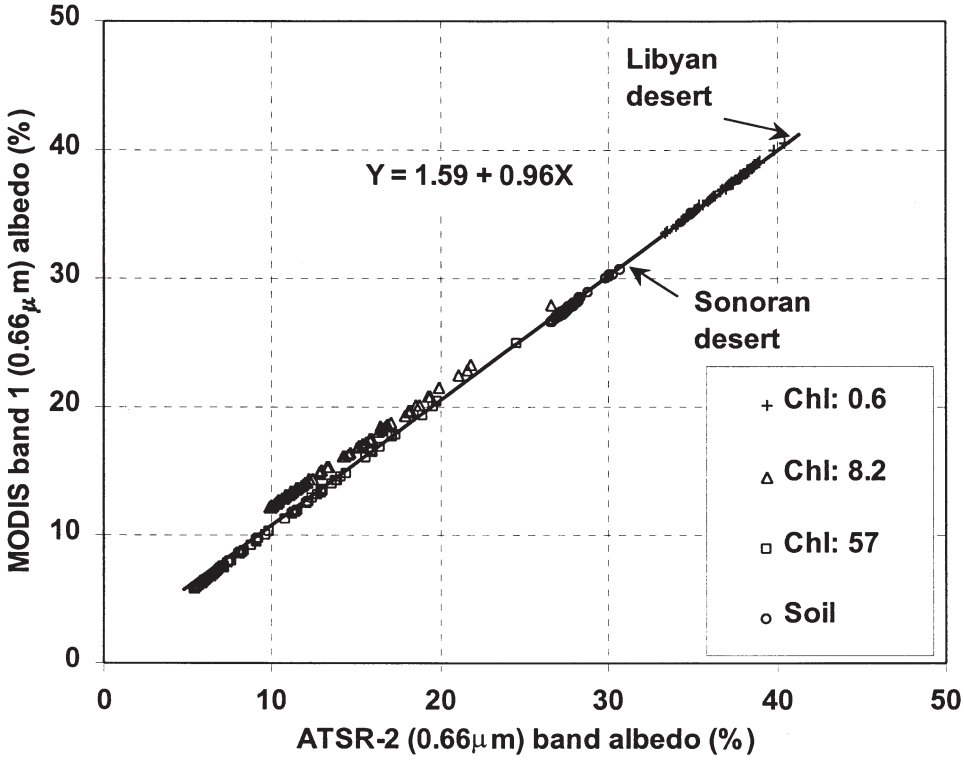


Figure 5. Regression of the computed MODIS band 1 albedo on the computed ATSR-2 0.66 $\mu$m band albedo.

pixels. A general sense of agreement between the measured and estimated MODIS and ATSR-2 albedos is apparent. We use the relative differences between the measured MODIS and ATSR-2 albedos as a measure of the efficacy of the inter-calibration of MODIS and ATSR-2. Accordingly, the relative difference between the measured MODIS and ATSR-2 albedos, A(measured), is defined as:

$$\text{A(measured)} = [\text{A(ATSR-2)} - \text{A(MODIS measured)}]/\text{A(ATSR-2)} \quad (5)$$

Similarly, we use the relative difference between the measured and estimated MODIS TOA albedos as a measure of the efficacy of our modelling. The relative difference A(estimated) is defined as:

$$\text{A(estimated)} = [\text{A(measured)} - \text{A(estimated)}]/\text{A(measured)} \quad (6)$$

A(measured) ranges from $-2.0\%$ to $+3.6\%$ when measurements on individual days are considered; similarly, A(estimated) ranges from $-3.0\%$ to $+4.3\%$. However, when the three-day mean MODIS albedo values over the two sites for a given channel are considered, there is noticeable improvement in the degree of correspondence between the two instruments, and between the estimated and measured MODIS albedos. We list in table 5 the relative differences between the mean values of MODIS and ATSR-2 measurements, and between the measured and estimated MODIS albedos. The reasonably low values of A(estimated) indicate that model-based, estimated albedos may be used as a surrogate calibration reference

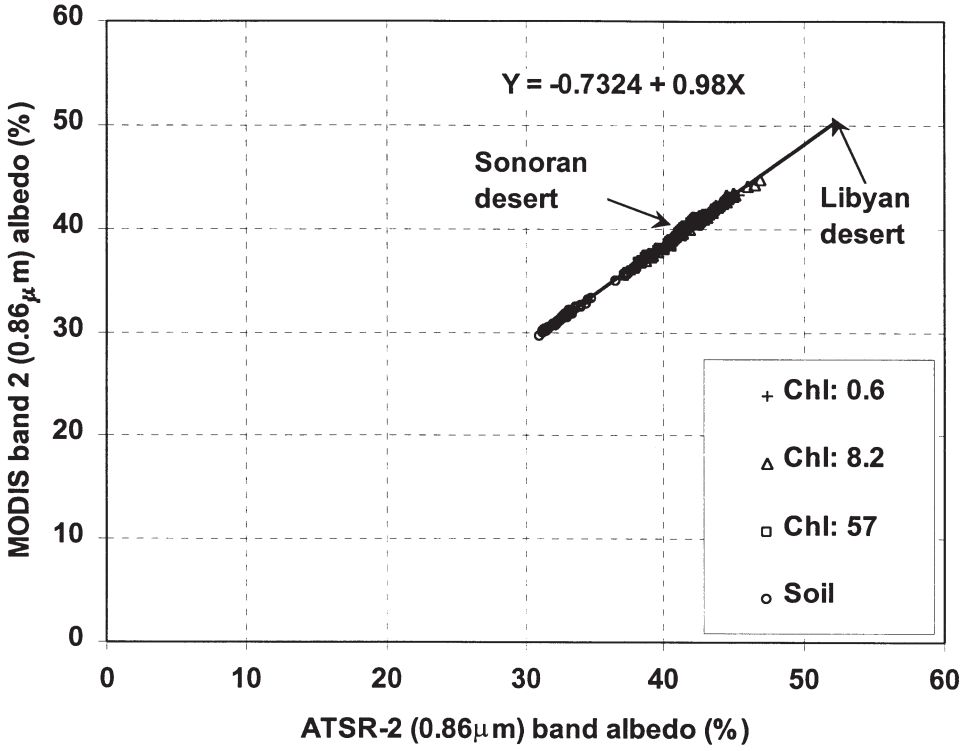


Figure 6. Regression of the computed MODIS band 2 albedo on the computed ATSR-2 0.86 $\mu$m band albedo.

Table 3. Inter-relationship between the MODIS and ATSR-2 albedos (%).

| X | Y | Regression equation | $R^2$ |
|---|---|---|---|
| ATSR-2 (0.56$\mu$m) | MODIS band 4 | $Y = X + 0.204$ | 0.990 |
| ATSR-2 (0.66$\mu$m) | MODIS band 1 | $Y = 0.960X + 1.590$ | 0.982 |
| ATSR-2 (0.86$\mu$m) | MODIS band 2 | $Y = 0.980X - 0.732$ | 0.987 |

(e.g. Teillet *et al.* 1990, Rao *et al.* 1997). The only noticeable departure from this pattern is the A(estimated) value for the Sonoran site in the 0.86 $\mu$m band. It should also be noted that all of the measured and estimated MODIS albedos are generally within one standard deviation of the mean of the measured ATSR-2 albedos.

The regression of the measured MODIS albedo on the estimated albedo (table 4) yields the following relationship between the two:

$$Y\ (\text{MODIS measured}) = 1.018 \times (\text{MODIS estimated}) - 0.216 \qquad (7)$$

with an $R^2$ value of 0.96 (figure 7). The above regression relationship clearly brings out the strong correspondence between the measured and estimated MODIS albedos, and reinforces the reasonableness of using model estimates to characterize the instrument in orbit.

The present results, and similar results for the post-launch calibration of the GOES imager using the AVHRR and ATSR-2 as calibration sources (Rao and

Table 4. Table of albedos (%).

| Site | Date | Wavelength ($\mu$m) | MODIS | | ATSR-2 measured |
|---|---|---|---|---|---|
| | | | Measured | Estimated | |
| Libyan desert (22°0′ N, 28°30′ E) | 29 December 2000 | 0.56 | 29.4 | 29.2 | 29.7 (3.0) |
| | | 0.66 | 42.4 | 43.8 | 44.0 (1.9) |
| | | 0.86 | 52.7 | 52.6 | 54.5 (2.3) |
| | 10 March 2001 | 0.56 | 30.2 | 29.2 | 29.7 (3.0) |
| | | 0.66 | 42.8 | 43.8 | 44.0 (1.9) |
| | | 0.86 | 53.0 | 52.6 | 54.5 (2.3) |
| | 26 March 2001 | 0.56 | 30.1 | 29.2 | 29.7 (3.0) |
| | | 0.66 | 43.7 | 43.8 | 44.0 (1.9) |
| | | 0.86 | 55.1 | 52.6 | 54.5 (2.3) |
| Sonora desert (32°0′ N, 114°6′ W) | 29 December 2000 | 0.56 | 24.3 | 24.4 | 24.2 (2.6) |
| | | 0.66 | 33.2 | 33.1 | 32.8 (2.5) |
| | | 0.86 | 41.5 | 39.7 | 41.3 (2.5) |
| | 12 March 2001 | 0.56 | 24.1 | 24.4 | 24.2 (2.6) |
| | | 0.66 | 33.1 | 33.1 | 32.8 (2.5) |
| | | 0.86 | 41.1 | 39.7 | 41.3 (2.5) |
| | 28 March 2001 | 0.56 | 24.4 | 24.4 | 24.2 (2.6) |
| | | 0.66 | 33.6 | 33.1 | 32.8 (2.5) |
| | | 0.86 | 41.6 | 39.7 | 41.3 (2.5) |

Note: The numbers in parentheses in the ATSR-2 column are the standard deviations of the albedo.

Table 5. Relative difference between measured and modelled albedos (MODIS: 3-day mean; ATSR-2: 3-year mean).

| Site | Wavelength ($\mu$m) | Albedo (%) | | | Relative difference (%) | |
|---|---|---|---|---|---|---|
| | | MODIS | | ATSR-2 | | |
| | | Measured | Estimated | | A(measured) | A(estimated) |
| Libyan desert | 0.56 | 29.9 | 29.2 | 29.7 | −0.7 | 2.3 |
| | 0.66 | 43.0 | 43.8 | 44.0 | 2.3 | −1.8 |
| | 0.86 | 53.6 | 52.6 | 54.5 | 1.7 | 1.9 |
| Sonoran desert | 0.56 | 24.3 | 24.4 | 24.2 | −0.4 | −0.4 |
| | 0.66 | 33.3 | 33.1 | 32.8 | −1.5 | 0.6 |
| | 0.86 | 41.4 | 39.7 | 41.3 | −0.2 | 4.1 |

Zhang, in preparation), indicate that similarity of the wavelength-dependent atmospheric and surface effects (e.g. gaseous and particulate absorption; surface reflection) in the spectral intervals covered by the two sensors being inter-calibrated is crucial to obtain meaningful results; the efficacy of inter-calibration is severely compromised if this requirement is not met (e.g. Rao and Sullivan 2001). The similarity requirement

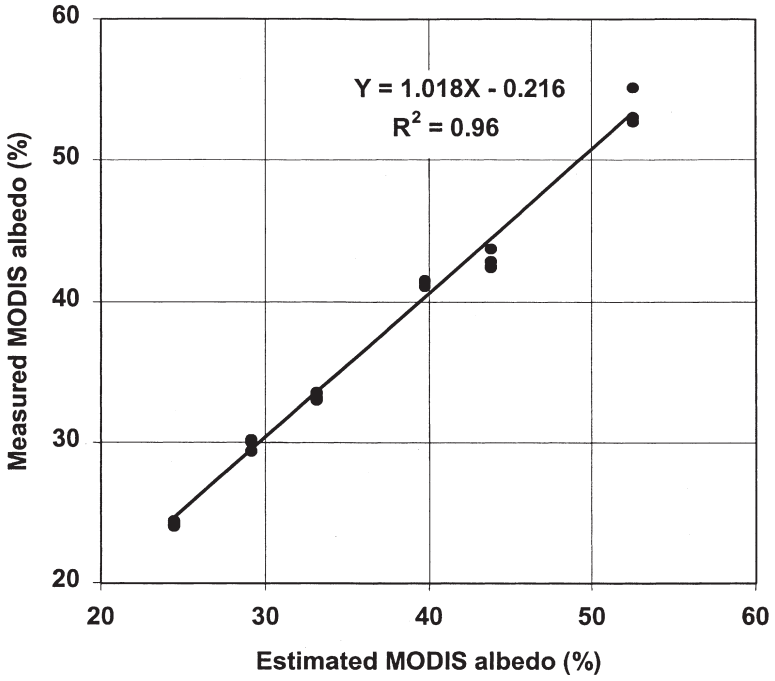


Figure 7. Regression of the computed MODIS albedo on the estimated values.

is generally met when the effective wavelengths of the two sensors to be inter-calibrated are close to each other, and their equivalent widths are comparable (table 1).

The reader may justifiably ask whether we can draw any meaningful conclusions regarding the performance of the MODIS on board calibrator based on a six-day record of measurements. Our main intent was to characterize the instrument as soon as practicable after operational data became available so that the users will have some basis to evaluate their products. Another point of concern is the assumption of a Lambertian surface in the model simulations; this assumption may limit the usefulness of our work to some degree. However, the very close correspondence between the measured and estimated MODIS TOA albedos, and the ATSR-2 albedos (§2.3; both near nadir and along-track) points to the adequacy of our model computations, especially when radiometric (reflectance) calibration accuracies of the order of 2–3% are required. Also, because of the sparsity of information on the bidirectional reflection properties of natural formations, and of the limited representativeness of the information presently available on a global scale, inclusion of the same in the model simulations may not provide discernibly better insight into the problem of inter-calibration of MODIS and ATSR-2.

## 4. Concluding remarks

We infer from a comparison of the estimated, modelled, and measured albedos in MODIS bands 1, 2 and 4, and in the 0.56 $\mu$m, 0.66 $\mu$m and 0.86 $\mu$m channels of ATSR-2 that the on board calibration of MODIS bands 1, 2 and 4 is performing as expected within the uncertainty (2%) associated with the ATSR-2 measurements.

We believe that MODIS and ATSR-2 can be used to monitor the in-orbit performance of each other, especially if the on board calibrator of either should fail. Model simulations of the inter-relationship between the MODIS and ATSR-2 TOA albedos can also be used as a secondary standard to characterize the in-orbit performance of the two instruments.

**Acknowledgments**

Work reported here was supported by the NOAA Office of Global Programs. The authors thank Drs J. T. Sullivan and M. P. Weinreb, NOAA/NESDIS Office of Research and Applications; and Drs P. Abel and W. Barnes, NASA Goddard Spaceflight Center, for a critical reading of the manuscript, and Dr Y. Kaufman of the same organization for comments on the results presented here. The ATSR-2 data were furnished by Dr D. L. Smith, Rutherford Appleton Laboratory, Didcot (United Kingdom).

**References**

Arriaga, A., and Schmetz, J., 1998, Calibration of the METEOSAT-5/-6 VIS channels with help of modelled radiances. *Contributions to Atmospheric Physics*, **72**, 133–139.

Berk, A., Bernstein, L. S., and Robertson, D. C., 1989, MODTRAN: A moderate resolution model for LOWTRAN 7, Report GL-TR-89-0122, Geophysics Laboratory, Air Force Systems Command, United States Air Force, Hanscom Air Force Base, MA 01731–5000.

Gao, B., 2000, A practical method for simulating AVHRR-consistent NDVI data series using narrow channels in the 0.5–1.0 $\mu$m spectral range. *IEEE Transactions on Geoscience and Remote Sensing*, **38**, 1969–1975.

Gitelson, A., and Merzlyak, M. N., 1994, Quantitative estimation of chlorophyll-a using reflectance spectra. *Journal of Photochemistry and Photobiology: B(Biology)*, **22**, 247–252.

Guenther, B., Barnes, W., Knight, E., Barker, J., Hamden, J., Weber, R., Roberto, M., Godden, G., Montgomery, H., and Abel, P., 1996, MODIS calibration: a brief review of the strategy for at-launch calibration approach. *Journal of Oceanic and Atmospheric Technology*, **13**, 274–285.

Kaufman, Y. J., and Holben, B. N., 1993, Calibration of the visible and near-IR bands of the AVHRR by atmospheric scattering, ocean glint, and desert reflection. *International Journal of Remote Sensing*, **14**, 21–52.

Rao, C. R. N. and Chen, J., 1995, Inter-satellite calibration linkages for the visible and near-infrared channels of the Advanced Very High Resolution Radiometer on the NOAA-7, -9, and -11 spacecraft. *International Journal of Remote Sensing*, **16**, 1931–1942.

Rao, C. R. N., and Sullivan, J. T., 2001, Calibration of the Advanced Very High Resolution Radiometer. In *Remote Sensing and Climate Change: Role of Earth observation*, edited by A. P. Cracknell (London: Springer-Praxis), pp. 117–157.

Rao, C. R. N., Chen, J., Sullivan, J. T., Zhang, N., and Wang, W., 1997, Vicarious calibration of meteorological satellite sensors in the visible and near-infrared regions of the spectrum. *Proceedings of the SPIE*, **3117**, 320–331.

Slater, P. N., Biggar, S. F., Thome, K. J., Gelman, D. L., and Spyak, P. R., 1996, Vicarious calibration of EOS sensors, *Journal of Oceanic and Atmospheric Technology*, **13**, 349–359.

Smith, D. L., Mutlow, C. T., and Rao, C. R. N., 2002, Calibration monitoring of the visible and near-infrared channels of the Along-Track scanning Radiometer-2 using stable terrestrial sites, *Applied Optics*, **41**, 515–523.

Staylor, W. F., 1990, Degradation rate of the AVHRR visible channel for the NOAA-6, -7, and -9 spacecraft. *Journal of Atmospheric and Oceanic Technology*, **7**, 411–423.

Teillet, P. M., Slater, P. N., Ding, Y., Santer, R. P., Jackson, R. D., and Moran, M. S., 1990, Three methods for the absolute calibration of the NOAA sensors in flight. *Remote Sensing of Environment*, **31**, 105–120.